

MULTI-RESPONSE OPTIMIZATION OF THERMOFORMING PARAMETERS FOR HYBRID BIODEGRADABLE CONTAINERS BASED ON CASSAVA LEAVES, SAWDUST, AND STARCH USING RESPONSE SURFACE METHODOLOGY

Chatree Homkhiew^{a*}, Chainarong Srivabutr^b, Worapong Boonchouytan^a

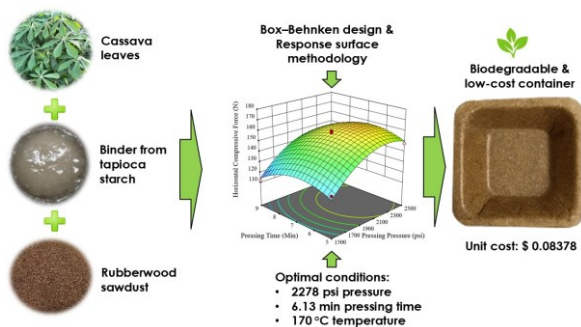
^aMaterials Processing Technology Research Unit, Department of Industrial Engineering, Faculty of Engineering, Rajamangala University of Technology Srivijaya, Muang, Songkhla, 90000, Thailand
^bDepartment of Industrial Engineering, Faculty of Engineering, Rajamangala University of Technology Srivijaya, Muang, Songkhla, 90000, Thailand

Article history

Received
3 May 2025
Received in revised form
28 July 2025
Accepted
30 July 2025
Published Online
16 June 2026

*Corresponding author
chatree.h@rmutsv.ac.th

Graphical abstract



Abstract

This study explores the optimization of thermoforming conditions to enhance the compressive performance of hybrid biodegradable containers fabricated from cassava leaves, sawdust, and starch via hot-compression molding. Using a Box-Behnken design integrated with response surface methodology, the effects of pressing pressure (1500-2500 psi), pressing time (5-9 minutes), and forming temperature (170-190 °C) on horizontal and vertical compressive forces were investigated. Regression analysis yielded statistically significant quadratic models for both responses with non-significant lack-of-fit, indicating model adequacy. Optimal forming conditions were determined to be 2278 psi pressure, 6.13 minutes pressing time, and 170 °C temperature, resulting in predicted compressive forces of 173 N (horizontal) and 41.27 N (vertical), with a maximum desirability score of 1.0. Experimental validation confirmed minimal deviation from predicted values. The findings demonstrate the potential of cassava leaf-sawdust-starch hybrid composites as sustainable raw materials for biodegradable packaging and highlight the effectiveness of statistically grounded optimization in improving mechanical performance through precise control of forming parameters.

Keywords: Cassava leaves, Hot-compression molding, Compressive strength, Box-Behnken design, Response surface methodology

© 2026 Penerbit UTM Press. All rights reserved

1.0 INTRODUCTION

The escalating environmental burden posed by synthetic packaging materials, particularly those

derived from non-biodegradable plastics, has catalyzed an urgent search for sustainable alternatives in the packaging industry [1]. Biodegradable packaging solutions, especially those derived from

renewable agricultural resources, have garnered increasing attention due to their potential to reduce environmental pollution, minimize fossil fuel dependency, and contribute to circular economy principles [2]. In this context, the valorization of agricultural residues into functional packaging products offers a promising pathway toward both environmental sustainability and value-added utilization of biomass. Among such residues, cassava leaves are abundantly available in tropical regions and traditionally treated as agricultural waste; however, they could be utilized as a novel raw material for developing biodegradable containers.

Despite the promising attributes of cassava leaves, their transformation into functional and mechanically stable containers requires careful control of the thermoforming process parameters. Forming techniques, such as hot-compression molding, offer the capability to shape natural fibers under heat and pressure, thereby facilitating the development of rigid bio-composite structures suitable for packaging applications. Nonetheless, the mechanical strength of such containers is inherently sensitive to variations in processing conditions, including forming temperature, pressure, and time. Achieving an optimal balance among these parameters is crucial for ensuring the structural integrity and functional performance of the final product. However, the complex interaction between these factors presents a significant challenge in developing standardized, scalable, and reliable production for cassava leaf-based containers.

Previous studies in the field of biodegradable packaging have primarily focused on materials such as starch, cellulose, and plant fibers from sources like banana, areca palm, or sugarcane bagasse [3]. For example, Islam *et al.* (2025) [4] extracted cellulose from coconut coir waste and fabricated eco-friendly food containers such as bowls, boxes, and plates, while Jahroo *et al.* (2021) [5] presented a method for producing biodegradable food packaging by combining abaca fiber pulp with wax coatings to enhance water resistance, and Putri *et al.* (2022) [6] investigated the production of biodegradable planting containers from oil palm empty fruit bunch fibers, demonstrating strong mechanical integrity and composability. However, limited attention has been given to cassava leaves, particularly in the context of optimizing the forming conditions for performance-driven applications. Furthermore, most existing works do not systematically explore the multi-response optimization of forming parameters with respect to key mechanical and functional properties such as horizontal and vertical compressive performances. This lack of targeted optimization hinders the practical applicability of cassava leaf-based containers and limits their potential as commercially viable alternatives to conventional packaging.

In addressing this research gap, the present work applies the Box-Behnken design (BBD) integrated with Response Surface Methodology (RSM) to systematically investigate and optimize the forming conditions, namely pressure, temperature, and time of

cassava leaf-based containers produced through hot-compression molding. In previous studies, the RSM was successfully applied to optimize process parameters. For example, Belwal *et al.* (2016) [7] used RSM to optimize extraction conditions for phenolic compounds and antioxidant activity in Berberis asiatica fruits. The methodology significantly improved bioactive yield through statistical modeling of temperature and solvent concentration variables. Said and Amin (2015) [8] emphasized the role of RSM in optimizing extraction processes, especially using Box-Behnken designs. It is helpful for applications in food, pharmaceutical, and herbal extraction industries. Mohamad *et al.* (2021) [9] employed RSM to optimize the adsorption performance of spent coffee grounds biochar for malachite green removal. Likewise, Priyatharishinia and Mokhtar (2020) [10] applied RSM to maximize the efficiency of the coagulant with central composite design (CCD), as well as analysing the effects of interaction between process factors. Yanis *et al.* (2019) [11] used RSM in predicting and optimization of cutting force and surface roughness of thin walled titanium alloys. More recently, Navale *et al.* (2023) [12] investigated the nonlinear lateral response of pile groups in clay using a parametric modeling approach to evaluate the effects of soil modulus and pile geometry, while Hasan *et al.* (2024) [13] optimized blast resistance performance of sandwich concrete bunkers through parametric simulation and predictive modeling. Therefore, these studies collectively underscore the effectiveness of response surface and parametric methods for analyzing complex process-response relationships. The present work expands this methodological framework into the realm of biodegradable hybrid composites, offering a novel application in sustainable packaging. It specifically models nonlinear interactions among forming parameters and their combined effects on two critical response variables: horizontal and vertical compressive forces. The outcome is a statistically optimized forming strategy that improves the mechanical integrity of agro-waste-based containers.

This research aims to develop biodegradable containers using cassava leaves, rubberwood sawdust, and starch-based binder, with a primary focus on achieving sufficient compressive force to support practical food-packaging applications. Specifically, it investigates the effects of key forming parameters, pressing pressure, pressing time, and forming temperature, on the mechanical performance of the containers, with the ultimate goal of optimizing the forming conditions for maximum strength and structural integrity.

The contributions of this study are twofold. First, it introduces cassava leaves as a novel, abundant, and sustainable raw material for bio-based packaging, expanding the range of renewable resources available for green product innovation. Second, it establishes a statistically robust optimization framework, based on response surface methodology and Box-Behnken design, to enhance the mechanical properties of molded bio-composite containers. These

findings provide critical insights into scalable production strategies for environmentally friendly packaging with commercial viability.

2.0 METHODOLOGY

2.1 Materials

The cassava leaves of the Hanatee cassava cultivar, which were used as the primary raw material and sourced from cassava plantations located in Songkhla Province, Thailand. Rubberwood sawdust, which was obtained from a rubberwood furniture manufacturing facility in Songkhla Province, Thailand and was employed to enhance the formability of the mixture. Chemical compositions of both cassava leaves and rubberwood were indicated in Table 1. Further, a premium quality tapioca starch (Red Cat brand) which was procured from Kriangkrai Company Limited and was utilized as a binding agent within the composition formulation.

The selection of cassava leaves as primary fiber is supported by their high cellulose content and availability as agricultural waste. Rubberwood sawdust has been demonstrated to enhance mechanical properties when used as a natural filler, especially at optimal loading levels, improving hardness and modulus while maintaining cost-effectiveness [14]. Further, tapioca starch, a widely available biodegradable polysaccharide, functions effectively as a binder, promoting interfacial adhesion between hydrophilic fibers and forming a cohesive composite structure; this is consistent with previous studies on starch-based natural fiber composites [15]. Together, these components form a synergistic combination: cassava leaves for fiber reinforcement, rubberwood sawdust for structural reinforcement and cost reduction, and tapioca starch as a natural binder, aligning with established methods in agro-waste-based biocomposite development.

Table 1 Chemical compositions of cassava leaves and rubberwood

| Raw material | Chemical composition (%) | | |
|---------------------|--------------------------|---------------|--------|
| | Cellulose | Hemicellulose | Lignin |
| Cassava leaves [16] | 22.6 | 16.9 | 7.6 |
| Rubberwood [17] | 39 | 29 | 28 |

2.2 Experimental Design to Optimize Condition

Experimental design is a vital statistical approach that minimizes variability, reduces the number of trials, and conserves resources such as time, cost, materials, and labor. The BBD is an efficient method for modeling second-order polynomial response surfaces and identifying optimal conditions [18]. As a spherical or nearly rotatable quadratic design without embedded factorial points, BBD places experimental runs at the center and midpoints of the variable space edges

[19]. Further, the RSM is employed to analyze multivariable systems, quantify factor effects, and explore complex interactions through statistical modeling [20], [21].

In this study, BBD was used to design the experiments and facilitate statistical analysis, while RSM was applied to develop regression models and perform multi-response optimization using Design-Expert software (Stat-Ease Inc., Minneapolis). The design incorporated three independent variables: pressing pressure (x_1 : 1500-2500 psi), pressing time (x_2 : 5-9 minutes), and forming temperature (x_3 : 170-190 °C), as detailed in Table 2. These variables, determined from prior studies and literature, significantly influence the compression force of cassava leaf-based containers. A total of 17 experimental runs, including 5 center and 12 factorial points, were executed to optimize two responses, as shown in Table 3. RSM was then employed to fit a second-order polynomial model to the data, as expressed in Eq. (1):

$$Y_{\text{predicted}} = \beta_0 + \sum_{i=1}^k \beta_i X_i + \sum_{i=1}^k \beta_{ii} X_i^2 + \sum_{i < j=2}^k \sum \beta_{ij} X_i X_j + \varepsilon_i \quad (1)$$

where Y is the predicted response; k , the number of factors; x_i and x_j , the independent variables; β_0 , the intercept; β_i , the linear coefficients; β_{ii} , the quadratic coefficients; β_{ij} , the interaction coefficients; and ε_i , the experimental error.

Table 2 Independent variables along with their constraints employed in the Box–Behnken design of experiments

| Independent factor | ID | Parameter level | | |
|-------------------------|-------|-----------------|------------|-----------|
| | | Low (-1) | Medium (0) | High (+1) |
| Pressing pressure (psi) | x_1 | 1500 | 2000 | 2500 |
| Pressing time (Min.) | x_2 | 5 | 7 | 9 |
| Temperature (°C) | x_3 | 170 | 180 | 190 |

2.3 Manufacturing Process for Cassava Leaf-based Containers

The production of containers from cassava leaves involved three main stages: raw material preparation, binder preparation, and hot-press forming.

In the raw material preparation stage, cassava leaves were first dried to remove moisture content to 4-5% and then manually sorted to eliminate large stems. The dried leaves were coarsely ground and sieved using a 12-mesh (1.68 mm opening) screen to ensure uniform particle size. Rubberwood sawdust was oven-dried at 120 °C for 8 hours to reduce moisture content to 4-5%, followed by sieving through the same mesh size to achieve consistency in particle dimensions [22].

For binder preparation, 125 g of tapioca starch was mixed with 500 mL of water and heated over low heat (approximately 65-70 °C) until the mixture became translucent, indicating gelatinization. The binder was then allowed to cool to room temperature before being incorporated with the fiber mixture.

In the forming stage, crushed cassava leaves (75 g) and rubberwood sawdust (25 g) were thoroughly dry-blended to obtain a 100 g fiber mixture with a 75:25 weight ratio. This mixture was combined with 50 mL of the prepared starch-based binder and kneaded manually for approximately 3 minutes until a homogeneous composite paste was obtained. A total of 65 g of the composite was weighed and placed into a carbon steel (S50C) mold with cavity dimensions of 110 mm × 110 mm × 3.6 mm (length × width × thickness), as shown in Figure 1. Prior to forming, the inner surfaces of the mold were lightly coated with vegetable oil to prevent adhesion of the binder to the mold during hot pressing. Forming was performed using a hot-press machine under the conditions specified in Table 3. The pressure was controlled via the hydraulic system and set directly in psi units using the machine's pressure gauge. After pressing, the molded container was demolded, and excess edges were trimmed. The final cassava leaf-based container is shown in Figure 2(a).



Figure 1 Carbon steel mold system used in the forming process

Table 3 Experimental conditions based on Box–Behnken design and observed response values

| Run no. | Actual parameter | | | Coded value | | | Response | |
|---------|------------------|-------|-------|-------------|-------|-------|----------|---------|
| | x_1 | x_2 | x_3 | x_1 | x_2 | x_3 | HCF (N) | VCF (N) |
| 1 | 1500 | 7 | 170 | -1 | 0 | -1 | 135 | 15.33 |
| 2* | 2000 | 7 | 180 | 0 | 0 | 0 | 155 | 36.46 |
| 3 | 1500 | 7 | 190 | -1 | 0 | +1 | 121 | 16.82 |
| 4* | 2000 | 7 | 180 | 0 | 0 | 0 | 159 | 35.82 |
| 5 | 2000 | 5 | 190 | 0 | -1 | +1 | 138 | 28.33 |
| 6 | 1500 | 5 | 180 | -1 | -1 | 0 | 125 | 10.88 |
| 7 | 2000 | 9 | 190 | 0 | +1 | +1 | 140 | 25.44 |
| 8 | 2000 | 5 | 170 | 0 | -1 | -1 | 161 | 36.96 |
| 9 | 2500 | 7 | 170 | +1 | 0 | -1 | 173 | 38.14 |
| 10 | 2500 | 5 | 180 | +1 | -1 | 0 | 148 | 30.59 |
| 11* | 2000 | 7 | 180 | 0 | 0 | 0 | 160 | 36.37 |
| 12 | 2500 | 9 | 180 | +1 | +1 | 0 | 145 | 27.08 |
| 13 | 2500 | 7 | 190 | +1 | 0 | +1 | 142 | 31.03 |
| 14 | 2000 | 9 | 170 | 0 | +1 | -1 | 145 | 31.61 |
| 15* | 2000 | 7 | 180 | 0 | 0 | 0 | 158 | 37.08 |
| 16* | 2000 | 7 | 180 | 0 | 0 | 0 | 157 | 34.43 |
| 17 | 1500 | 9 | 180 | -1 | +1 | 0 | 112 | 7.44 |

Note; * Duplicate experiments; HCF is horizontal compressive force, VCF is vertical compressive force, and N is newton.

2.4 Testing of Compressive Force

Horizontal and vertical compression tests were conducted to evaluate the horizontal and vertical load-bearing capacity of cassava leaf-based containers, which adapted from the ISO 3035 standard

for corrugated fibreboard. Testing was performed using a universal mechanical testing machine (Model NRI-TS500-50, Narin Instrument Co., Ltd.) at a compression rate of 5 mm/min, as illustrated in Figures 2(b) and 2(c). The length, width, and thickness of the formed biodegradable containers were measured using a digital vernier caliper with an accuracy of 0.01 mm. For each experimental run, three replicate specimens were fabricated under identical forming conditions.

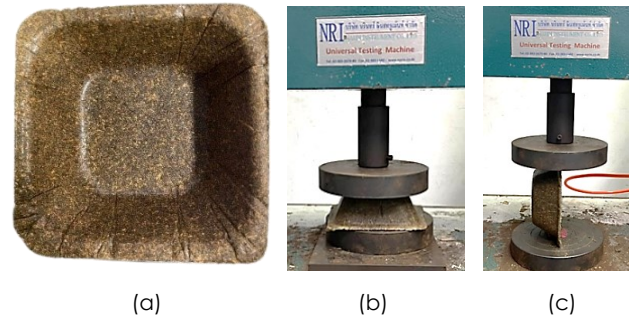


Figure 2 Visual representation of (a) cassava leaf-based container sample, (b) horizontal compressive test, and (c) vertical compressive test

3.0 RESULTS AND DISCUSSION

3.1 ANOVA for the Different Models Fitted to Responses

A Box–Behnken design with three independent variables was employed across 17 randomized experimental runs to evaluate two responses: horizontal compressive force (HCF) and vertical compressive force (VCF), as presented in Table 3. Model fitting results indicated that all responses were best described by quadratic models, outperforming linear, two-factor interaction (2FI), and cubic alternatives. These models showed statistically significant sequential sums of squares ($p < 0.05$), non-significant lack of fit ($p > 0.05$), and high coefficients of determination, with adjusted R^2 (Adj- R^2) and predicted R^2 (Pred- R^2) values approaching 100% [23]. For instance, the HCF model yielded a p -value of < 0.0001 for sequential sums of squares, a non-significant lack of fit ($p = 0.1339$), an adjusted R^2 of 97.09%, and a predicted R^2 of 84.80%, indicating strong model adequacy [24].

Analysis of variance (ANOVA) for each response (Table 4) confirmed the statistical significance of the fitted models ($p < 0.05$). Among the main effects, pressing pressure (x_1), pressing time (x_2), and temperature (x_3) significantly influenced both responses. However, several interaction terms were statistically insignificant, including pressing pressure (x_1) × pressing time (x_2) for HCF; pressing pressure (x_1) × pressing time (x_2) and pressing time (x_2) × temperature (x_3) for VCF. Such interactions are typically analyzed using the RSM [25]. Additionally, second-order terms for temperature (x_3^2), in both HCF and VCF models, were

also non-significant. Following recommendations by Petdee et al. (2023) [26], these terms were removed to improve model performance, as eliminating insignificant terms enhances the predicted R^2 value.

Table 4 ANOVA for the quadratic response surface models corresponding to each property of cassava leaf-based containers

| Source | Horizontal compressive force | | Vertical compressive force | |
|-----------------|------------------------------|----------|----------------------------|----------|
| | F-value | p-value | F-value | p-value |
| Model | 60.29 | <0.0001* | 77.19 | <0.0001* |
| x_1 | 229.21 | <0.0001* | 330.79 | <0.0001* |
| x_2 | 14.99 | 0.0061* | 13.09 | 0.0085* |
| x_3 | 88.73 | <0.0001* | 23.65 | 0.0018* |
| x_1x_2 | 3.33 | 0.1108 | 0.0006 | 0.9818 |
| x_1x_3 | 9.62 | 0.0173* | 8.39 | 0.0231* |
| x_2x_3 | 10.79 | 0.0134* | 0.6864 | 0.4347 |
| x_1^2 | 114.29 | <0.0001* | 237.29 | <0.0001* |
| x_2^2 | 68.17 | <0.0001* | 66.27 | <0.0001* |
| x_3^2 | 0.3369 | 0.5798 | 0.3745 | 0.5599 |
| Lack of fit | 3.40 | 0.1339 | 3.80 | 0.1149 |
| R^2 (%) | 98.73 | | 99.00 | |
| Adj- R^2 (%) | 97.09 | | 97.72 | |
| Pred- R^2 (%) | 84.80 | | 87.78 | |

Note; *A p-value < 0.05 indicates statistical significance.

Table 5 presents the ANOVA results for the reduced quadratic models of the HCF and VCF responses. All model terms were statistically significant ($p < 0.05$), and the lack-of-fit tests were non-significant ($p > 0.05$), confirming the models' adequacy [27]. Model performance was further validated using statistical indicators including R^2 , adjusted R^2 , and predicted R^2 . The R^2 values for HCF and VCF were 98.06% and 98.85%, respectively, indicating that over 98% of the variance in the data was captured by the models. The high adjusted R^2 and predicted R^2 values, ranging from 88.17% to 98.16%, further confirm model reliability and predictive capability, with the VCF model achieving the highest pred- R^2 of 94.27%, reflecting minimal unexplained variability in new predictions [28], [29], [30]. The final regression equations, derived using Design-Expert software, are presented in Eqs. (2)-(3), expressed in terms of actual factor levels.

$$\text{HCF} = -109.76 + 0.411x_1 - 3.645x_2 - 0.787x_3 - 0.00085x_1x_3 + 0.225x_2x_3 - 0.000057x_1^2 - 2.766x_2^2 \quad (2)$$

$$\text{VCF} = -353.98 + 0.274x_1 + 19.583x_2 + 0.605x_3 - 0.00043x_1x_3 - 0.000044x_1^2 - 1.467x_2^2 \quad (3)$$

3.2 Model Adequacy Evaluation

Diagnostic plots in Figures 3 and 4 including normal probability and residuals versus predicted values, were evaluated to validate the model fit. Figures 3(a) and 4(a) show the normal probability plot of residuals for HCF and VCF, respectively, where the points closely follow a straight line, indicating normal distribution and confirming model adequacy. According to Myers et al. [28], a good fit is characterized by such alignment

with minimal scattering [31]. In the residuals versus predicted plot (Figures 3(b) and 4(b)), all externally studentized residuals fall within control limits and exhibit random distribution, with no discernible patterns, supporting the model's appropriateness. Thus, these diagnostic results confirm that the fitted quadratic models for HCF and VCF are reliable. Further, Figures 3(c) and 4(c) illustrate the correlations between actual and predicted responses for HCF and VCF, respectively, based on model equations (2)-(3). In all cases, the data points align closely along the 45° line, with deviations under 5%, indicating strong predictive accuracy and model adequacy for all two responses.

Table 5 ANOVA for the reduced quadratic response surface models corresponding to each property of cassava leaf-based containers

| Source | Horizontal compressive force | | Vertical compressive force | |
|-----------------|------------------------------|----------|----------------------------|----------|
| | F-value | p-value | F-value | p-value |
| Model | 64.96 | <0.0001* | 143.41 | <0.0001* |
| x_1 | 185.79 | <0.0001* | 410.33 | <0.0001* |
| x_2 | 12.64 | 0.0062* | 16.23 | 0.0024* |
| x_3 | 74.87 | <0.0001* | 29.34 | 0.0003* |
| x_1x_3 | 8.12 | 0.0191* | 10.41 | 0.0091* |
| x_2x_3 | 9.10 | 0.0145* | - | - |
| x_1^2 | 97.25 | <0.0001* | 293.93 | <0.0001* |
| x_2^2 | 58.11 | <0.0001* | 81.78 | <0.0001* |
| Lack of fit | 3.53 | 0.1228 | 2.29 | 0.2212 |
| R^2 (%) | 98.06 | | 98.85 | |
| Adj- R^2 (%) | 96.55 | | 98.16 | |
| Pred- R^2 (%) | 88.17 | | 94.27 | |

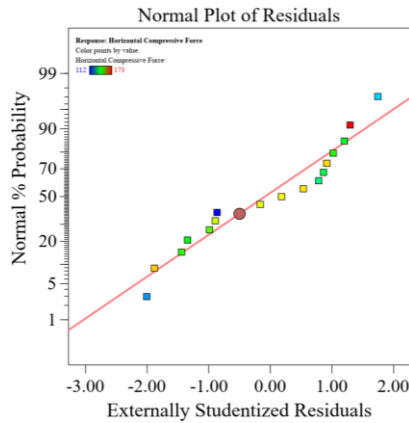
Note; *A p-value < 0.05 indicates statistical significance.

3.3 Effects of Forming Condition on Horizontal Compressive Force, and Optimal Condition

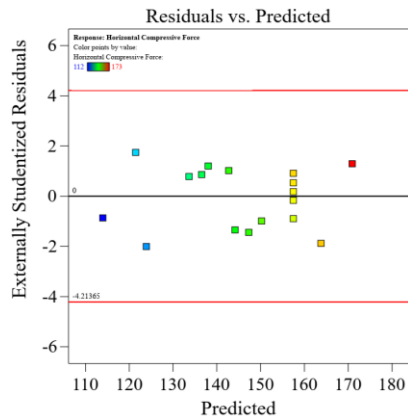
Based on the regression model for horizontal compressive force, the three-dimensional response surface plots in Figure 5 illustrate the effect of pressing pressure (x_1), pressing time (x_2), and temperature (x_3) on the horizontal compressive performance of cassava leaf-based containers. Pressing pressure in the range of 1500-2300 psi contributed positively to horizontal compressive resistance, likely due to improved particle compaction and interfacial adhesion. However, when the pressure exceeded 2300 psi, a decline in resistance was observed. Excessive pressure could be led to internal defects such as microcracking or non-uniform porosity, which adversely affected structural strength. Further, the decrease in container height observed at high forming pressures can be attributed to over-compaction of the fiber-binder matrix. Under excessive pressure, the starch-based binder becomes plastically deformable due to heat, and the solid content flows laterally within the mold cavity. This causes the vertical structure to compress, reducing the final height.

An increase in pressing time up to approximately 5-7 minutes significantly enhanced horizontal compressive resistance. This duration appeared sufficient for heat penetration and structural consolidation of the material. However, further

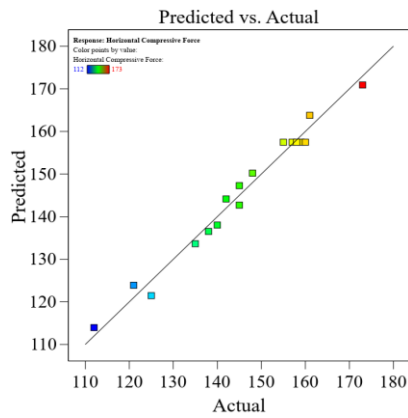
extension beyond 7 minutes resulted in a notable decrease in compressive force. This deterioration was associated with cumulative thermal effects, where prolonged exposure, even under constant temperature, led to thermal aging and degradation of the organic matrix. As pressing time increased, so does internal heat build-up, accelerating the breakdown of starch and fibrous components, thereby weakening the composite's structural performance [32].



(a)



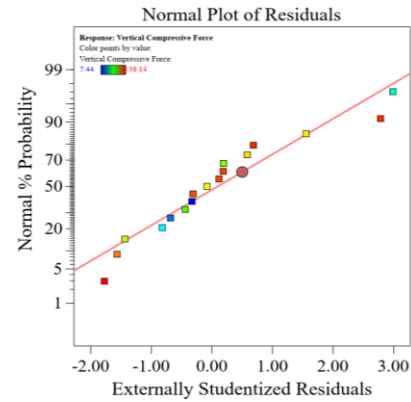
(b)



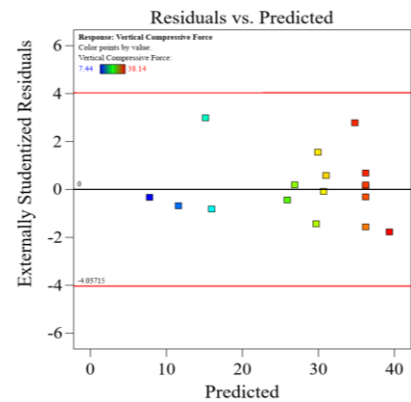
(c)

Figure 3 Model adequacy evaluation for horizontal compressive force: (a) normal probability plot of residuals, (b) residuals versus predicted values, and (c) predicted versus observed values

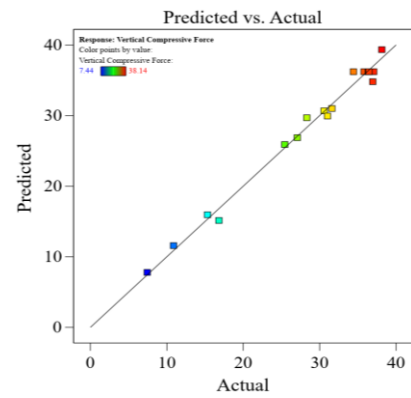
Further, within the pressing pressure range of 1500-2100 psi, increasing the forming temperature led to a gradual reduction in horizontal compressive resistance. However, when the pressure exceeded 2100 psi, the decrease in horizontal compressive resistance became more pronounced. This trend was attributed to the thermal degradation of natural components, particularly cassava leaves and rubberwood sawdust, as well as tapioca starch, which functions as the primary binder in the composite matrix. At elevated temperatures, starch undergoes structural breakdown, diminishing its binding efficiency and compromising the mechanical integrity of the composite material [33].



(a)



(b)



(c)

Figure 4 Model adequacy evaluation for vertical compressive force: (a) normal probability plot of residuals, (b) residuals versus predicted values, and (c) predicted versus observed values

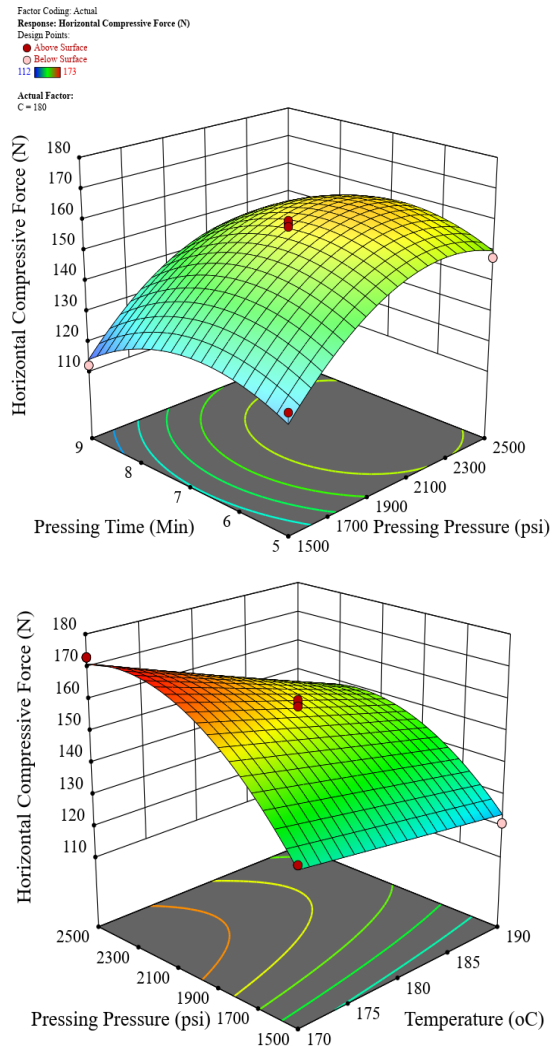


Figure 5 Three-dimensional response surface plots showing the influence of forming parameters on horizontal compressive force of cassava leaf-based containers

The results indicated that optimal forming condition required a careful balance between pressing pressure, pressing time, and temperature. Deviations beyond the critical limits of these parameters can cause thermal degradation or mechanical over-compaction, ultimately reducing the mechanical integrity of cassava leaf-based containers. Understanding these interdependencies are essential for optimizing process parameters and ensuring consistent product performance. In addition, response surface optimization was also employed to identify the optimal forming condition for maximizing horizontal compressive force of the cassava leaf-based containers, using Design-Expert software under default settings to generate a desirability score. Based on the fitted quadratic model, the optimal condition was summarized in Table 6, which included a pressing pressure of 2360 psi, pressing time of 6.3 minutes, and forming temperature of 170 °C, achieving a maximum

desirability of 1.000. The corresponding predicted HCF value was 173 N.

Table 6 Predicted responses for each property using the optimized forming parameters

| Property | Variable parameter | | | Predicted response | Desirability |
|------------------------------|--------------------|----------------|----------------|--------------------|--------------|
| | X ₁ | X ₂ | X ₃ | | |
| Horizontal compressive force | 2360 | 6.3 | 170 | 173 N | 1.000 |
| Vertical compressive force | 2185 | 6.8 | 178 | 38.81 N | 1.000 |

3.4 Effects of Forming Condition on Vertical Compressive Force, and Optimal Condition

Figure 6 showed the three-dimensional response surface plots based on the regression model of vertical compressive force. It demonstrated how pressing pressure, pressing time, and temperature influenced the vertical compressive behavior of cassava leaf-based containers. The pressing pressure between 1500 and 2200 psi enhanced vertical compressive resistance, likely due to improved particle densification and interfacial bonding. However, beyond 2200 psi, a decline in resistance was observed, possibly due to the formation of internal flaws such as microcracks that compromised structural integrity. Further, a pressing time of 5 to 6.5 minutes significantly improved vertical compressive performance, suggesting that this duration allowed adequate heat transfer. In contrast, pressing times exceeding 6.5 minutes resulted in a marked reduction in vertical compressive force. This decline could be attributed to prolonged thermal exposure, which accelerates the degradation of starch and lignocellulosic components.

In addition, the forming temperature exhibited a complex interaction with pressing pressure. Within the 1500–1850 psi range, increasing temperature gradually reduced vertical compressive resistance. This reduction became more pronounced at pressures above 1850 psi, indicating the onset of thermal degradation. The diminished mechanical strength was attributed to the breakdown of natural components, particularly cassava leaves, rubberwood sawdust, and tapioca starch, under elevated temperatures. As starch, the primary binder in the composites, loses its structural integrity at high temperatures, its binding efficiency deteriorates, adversely affecting the overall mechanical performance [33].

The observed interactions suggested that optimal mechanical performance depends not solely on individual parameters but on their synergistic effects. For instance, an increase in pressing time that may be beneficial at lower temperatures becomes detrimental at higher temperatures due to accumulated thermal stress. Similarly, while moderate pressure enhanced

fiber cohesion, excessive pressure could induce physical damage or alter porosity, counteracting its benefits. To further optimize the forming parameters, response surface methodology was applied using Design-Expert software with default settings to compute the desirability score. The optimal forming condition for vertical compressive force, derived from the fitted quadratic model, was summarized in Table 6. It included a pressing pressure of 2185 psi, pressing time of 6.8 minutes, and forming temperature of 178 °C. This condition yielded a maximum desirability score of 1.000, with the predicted vertical compressive force of 38.81 N. These optimized parameters provide a practical guideline for scaling up the production of cassava leaf-based containers with enhanced structural integrity, while also offering insight into the thermal and mechanical behavior of bio-based materials during compression molding. Future work may investigate long-term durability, moisture sensitivity, and life-cycle performance under real-world usage conditions.

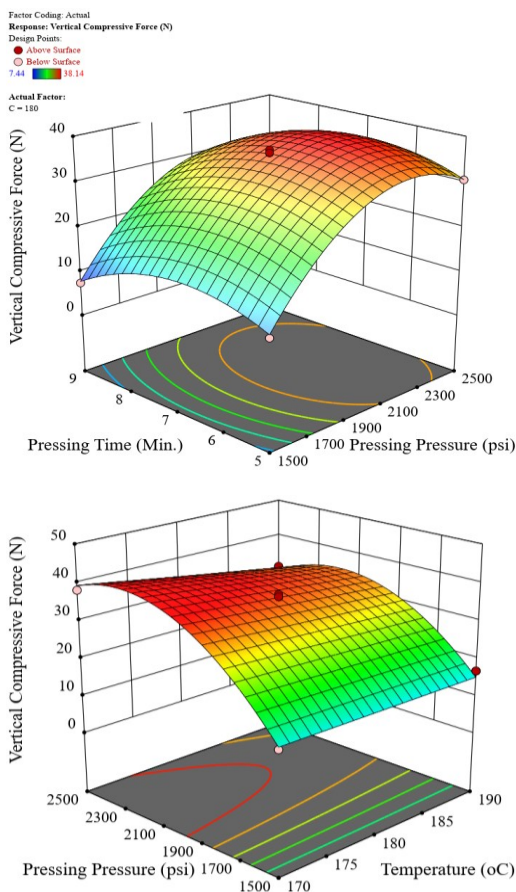


Figure 6 Three-dimensional response surface plots showing the influence of forming parameters on vertical compressive force of cassava leaf-based containers

3.5 Optimal Forming Condition of Cassava Leaf-Based Containers

The optimal forming condition of cassava leaf-based containers was determined using numerical

optimization via the desirability function in Design-Expert software. Optimization criteria consisted three input parameters: pressing pressure, pressing time, and temperature within the experimental range, and two response variables: maximum horizontal and vertical compressive forces. A desirability value near 1.0 indicates a highly favorable outcome [34], [35]. The ramp function plots in Figure 7 illustrates response behavior and desirability across design space. The optimal condition yielded a desirability score of 1.0 (100%), with predicted responses of 173 N (horizontal compressive force) and 41.27 N (vertical compressive force). The optimal forming parameters were 2278 psi pressing pressure, 6.13 minutes, pressing time, and 170 °C forming temperature.

Model validation was performed by conducting experiments at the predicted optimal condition. The experimental results (Table 7) closely matched the predicted values, with minimal deviation across all responses. The lowest deviation was observed in horizontal compressive force, at 1.15%, confirming the adequacy of the regression models.

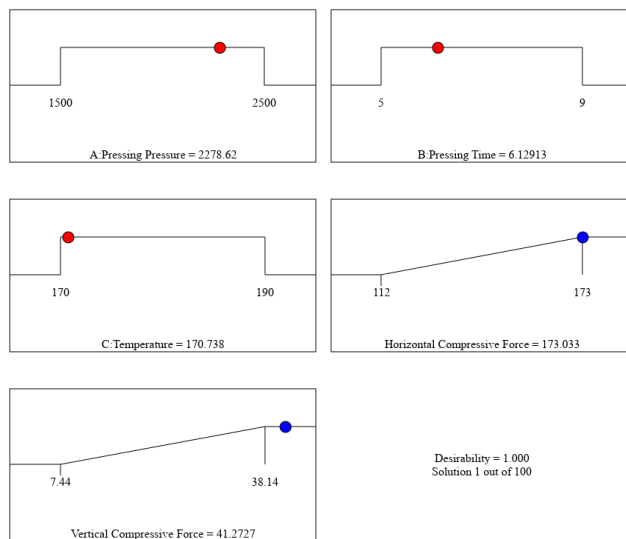


Figure 7 Predicted optimal forming conditions and corresponding compressive force responses, with a maximum overall desirability of 1.0

Table 7 Predicted versus experimentally observed values for each response under the optimized conditions

| Response | Predicted value | Observed value* | Residual | Error (%) |
|----------------------------------|-----------------|-----------------|----------|-----------|
| Horizontal compressive force (N) | 173 | 171 (23) | 2 | 1.15 |
| Vertical compressive force (N) | 41.27 | 42.51 (5.8) | 1.24 | 3.0 |
| Desirability | 1.000 | | | |

Note: *The values in parentheses are standard deviations from three replicates.

3.6 Cost Estimation

When the new materials or products are successfully developed, the cost calculation of the products manufactured from such materials is necessary. Generally, the cost of product consists of seven main types: (1) direct material, (2) indirect material, (3) energy, (4) overhead, (5) depreciation, (6) direct labor, and (7) indirect labor. However, this work particularly explores the direct material cost and energy cost (or energy cost of processing) of a cassava leaf-based container with dimensions of 110 mm × 110 mm × 3.6 mm.

Direct material cost of the cassava leaf-based container. The materials used to produce the container include the three compositions; cassava leaves, rubberwood sawdust, and tapioca starch. The container is dimensions of 110 mm × 110 mm × 3.6 mm. Thus, the quantities of each material mixed are 18.75 g for cassava leaves, 6.25 g for rubberwood sawdust, and 31.25 g for tapioca starch, as shown in Table 8. Likewise, the prices of each material are 0.000029 USD/g for cassava leaves, 0.00014 USD/g for rubberwood sawdust, and 0.0012 USD/g for tapioca starch. Thus, the direct material cost of each material can be calculated by using Eq. (4):

$$\text{Cost}_{\text{material}} = \text{Quantity} \times \text{Price} \quad (4)$$

The total cost of direct materials is 0.03891 USD per piece.

Table 8 Direct material cost of the cassava leaf-based container

| Material | Quantity (g) | Price (USD/g) | Cost (USD) |
|--------------------------------|--------------|---------------|------------|
| Cassava leaves | 18.75 | 0.000029 | 0.00054 |
| Rubberwood sawdust | 6.25 | 0.00014 | 0.00087 |
| Tapioca starch | 31.25 | 0.0012 | 0.03750 |
| Total cost of direct materials | | | 0.03891 |

Energy cost in processing of the cassava leaf-based container. The production of the container products was included with four stage processes: (1) cassava leaf flour preparation, (2) rubberwood sawdust preparation, (3) binder preparation, and (4) forming process. The machines used in the preparing process are crushing machine, sieving machine, and oven, as shown in Table 9. The crushing machine, sieving machine, and oven used electric power are 1.5, 1.5, and 1.0 kW, respectively, and they were consumed 0.02, 0.01667, and 0.019 hour, respectively. Further, expense of electric energy for small business with voltage of 22-33 kV is 0.068 USD per unit. Thus, the energy cost of each machine can be calculated by using Eq. (5):

$$\text{Energy Cost}_{\text{processing}} = \text{Electric power} \times \text{Consumption} \times 0.068 \quad (5)$$

The total energy cost of processing is 0.04487 USD per piece.

The estimated cost of the cassava leaf-based container product with dimensions of 110 mm × 110 mm × 3.6 mm based on the summation of direct material cost and energy cost in processing is approximately 0.08378 USD per piece.

Table 9 Energy cost in processing of the cassava leaf-based container

| Machine | Electric power (kW) | Consumption (Hour) | Cost (USD) |
|--|---------------------|--------------------|------------|
| <i>(1) Preparation process of cassava leaf flour</i> | | | |
| Crushing machine | 1.5 | 0.02 | 0.00204 |
| Sieving machine | 1.5 | 0.01667 | 0.00170 |
| <i>(2) Preparation process of rubberwood sawdust</i> | | | |
| Sieving machine | 1.5 | 0.01667 | 0.00170 |
| Oven | 1.0 | 0.019 | 0.00129 |
| <i>(3) Binder preparation process</i> | | | |
| Electric pan | 1.0 | 0.05 | 0.00340 |
| <i>(4) Forming process</i> | | | |
| Hot press machine | 5.0 | 0.1022 | 0.03474 |
| Total energy cost in processing | | | 0.04487 |

4.0 CONCLUSION

This study successfully optimized the thermoforming parameters for cassava leaf-based biodegradable containers using BBD and RSM. Second-order polynomial models showed high predictive accuracy ($R^2 > 98\%$, desirability = 1.000). The optimal forming conditions for maximizing compressive forces were determined to be 2278 psi pressure, 6.13 minutes pressing time, and 170 °C forming temperature. Under these parameters, the cassava leaf-based containers achieved predicted compressive forces of 173 N (horizontal) and 41.27 N (vertical), with experimental validation confirming model reliability at a deviation of less than 3%. The results highlight that moderate forming conditions enhance fiber compaction and interfacial bonding, whereas excessive conditions induce thermal degradation and reduce mechanical properties. Additionally, the unit production cost was estimated at USD 0.08378, reinforcing the material's potential for commercial packaging applications. These findings contribute both theoretically, by offering a statistical optimization framework for agro-waste materials, and practically, by presenting a scalable, low-cost alternative aligned with circular economy goals. However, the study is limited to evaluating only compressive properties and a single mold design. Other important characteristics, such as tensile, flexural, impact resistance, and biodegradability, were not assessed. Future work should explore these aspects, as well as investigate material modifications (e.g., fiber treatment, plasticizer incorporation) to further enhance performance and applicability.

Acknowledgement

The authors would like to express their thanks to the Thailand Science Research and Innovation (Research Grant Code: 4696418) for financial support throughout this work, and the Rajamangala University of Technology Srivijaya (RUTS), Thailand.

Conflicts of Interest

The manuscript has not been published elsewhere and is not under consideration by other journals. All authors have approved the review, agree with its submission and declare no conflict of interest on the manuscript.

References

- [1] Ncube, L. K., A. U. Ude, E. N. Ogunmuyiwa, R. Zulkifli, and I. N. Beas. 2020. Environmental Impact of Food Packaging Materials: A Review of Contemporary Development from Conventional Plastics to Polylactic Acid Based Materials. *Materials*. 13(21): 4994. <https://doi.org/10.3390/ma13214994>.
- [2] Zhao, X., Y. Wang, X. Chen, X. Yu, W. Li, S. Zhang, X. Meng, Z.-M. Zhao, T. Dong, A. Anderson, A. Aiyedun, Y. Li, E. Webb, Z. Wu, V. Kunc, A. Ragauskas, S. Ozcan, and H. Zhu. 2023. Sustainable Bioplastics Derived from Renewable Natural Resources for Food Packaging. *Matter*. 6(1): 97–127. <https://doi.org/10.1016/j.matt.2022.11.006>.
- [3] Kóczán, Z., and Z. Pásztori. 2024. Overview of Natural Fiber-Based Packaging Materials. *Journal of Natural Fibers*. 21(1): 2301364. <https://doi.org/10.1080/15440478.2023.2301364>.
- [4] Islam, M. H., M. H. Ara, M. A. Khan, J. Naime, M. L. Rahman, T. A. Ruhane, and M. A. R. Khan. 2025. A Sustainable Approach for the Development of Cellulose-Based Food Container from Coconut Coir. *ACS Omega*. 10(1): 157–169. <https://doi.org/10.1021/acsomega.4c03031>.
- [5] Jahroo, W. L., M. D. C. A. Muhammad, and S. I. Sakina. 2021. Biodegradable Food Container Made of Abaca Fiber Pulp with Beeswax Biocoating. *Advances in Social Science, Education and Humanities Research*. 625: 195–200. <https://doi.org/10.2991/assehr.k.211228.025>.
- [6] Putri, Z. W., M. Lutfi, and D. Darmanto. 2022. The Utilization of Oil Palm Empty Fruit Bunches (OPEFB) for Biodegradable's Pot Raw Materials as an Alternative Container for Sustainable Nurseries. *Applied Research in Science and Technology*. 2(2): 84–99. <https://doi.org/10.33292/areste.v2i2.30>.
- [7] Belwal, T., P. Dhyani, I. D. Bhatt, R. S. Rawal, and V. Pande. 2016. Optimization Extraction Conditions for Improving Phenolic Content and Antioxidant Activity in *Berberis asiatica* Fruits Using Response Surface Methodology (RSM). *Food Chemistry*. 207: 115–124. <https://doi.org/10.1016/j.foodchem.2016.03.081>.
- [8] Mohamad Said, K. A., and M. A. Mohamed Amin. 2015. Overview on the Response Surface Methodology (RSM) in Extraction Processes. *Journal of Applied Science & Process Engineering*. 2(1): 8–17. <https://doi.org/10.33736/jaspe.161.2015>.
- [9] Mohamad, M., R. Wannahari, R. Mohammad, N. F. Shoparwe, W. L. Kwan, and J. W. Lim. 2021. Adsorption of Malachite Green Dye Using Spent Coffee Ground Biochar: Optimisation Using Response Surface Methodology. *Jurnal Teknologi (Sciences & Engineering)*. 83(1): 27–36. <https://doi.org/10.11113/jurnalteknologi.v83.14904>.
- [10] Priyatharishinia, M., and N. M. Mokhtar. 2020. Analysis of *Artocarpus heterophyllus* Peel as a Natural Coagulant Using Response Surface Methodology (RSM). *Jurnal Teknologi (Sciences & Engineering)*. 82(4). <https://doi.org/10.11113/jt.v82.14451>.
- [11] Yanisa, M., A. S. Mohrunia, S. Sharif, and I. Yani. 2019. Optimum Performance of Green Machining on Thin Walled Ti6Al4V Using RSM and ANN in Terms of Cutting Force and Surface Roughness. *Jurnal Teknologi (Sciences & Engineering)*, 81(6). <https://doi.org/10.11113/jt.v81.13443>.
- [12] Navale, A., S. Patil, and S. Mulani. 2023. Nonlinear Lateral Response of Pile Group in Clay Using the Modified Cam-Clay Soil Model. *Journal of Civil Engineering, Science and Technology*. 14(1): 1–13. <https://doi.org/10.33736/jcest.4909.2023>.
- [13] Hasan, M., and Kueh, A. 2024. Blasting Resistance of Curved Sandwich Composite Concrete Bunkers. *Structural Engineering and Mechanics*. 91(1): 63–75. <https://doi.org/10.12989/sem.2024.91.1.063>.
- [14] Homkhiew, C., E. Pianhanuruk, S. Rawangwong, W. Boonchouytan, and R. Numrat. 2020. Rubberwood Sawdust Filled Natural Rubber Composites: Effects of Filler Loading and Zinc Oxide Content. *IOP Conference Series: Materials Science and Engineering*. 773: 012005. <https://doi.org/10.1088/1757-899X/773/1/012005>.
- [15] Yusof, F. Md., N. A. Wahab, N. L. Abdul Rahman, A. Kalam, A. Jumahat, and C. F. Mat Taib. 2019. Properties of Treated Bamboo Fiber Reinforced Tapioca Starch Biodegradable Composite. *Materials Today: Proceedings*. 16(4): 2367–2373. <https://doi.org/10.1016/j.matpr.2019.06.140>.
- [16] Ravindran, V., P. Rajadevan, L. A. Goonewardene, and A. S. B. Rajaguru. 1986. Effects of Feeding Cassava Leaf Meal on the Growth of Rabbits. *Agricultural Wastes*. 17: 217–224.
- [17] Petchpradab, P., T. Yoshida, T. Charinpanitkul, and Y. Matsumura. 2009. Hydrothermal Pretreatment of Rubber Wood for the Saccharification Process. *Industrial and Engineering Chemistry Research*. 48(9): 4587–4591. <https://doi.org/10.1021/ie801314h>.
- [18] Raghupathy, R., and K. S. Amirthagadeswaran. 2014. Optimization of Casting Process Based on Box-Behnken Design and Response Surface Methodology. *International Journal of Quality Research*. 8(4): 569–582.
- [19] Zolgharnein, J., A. Shahmoradi, and J. B. Ghasemi. 2013. Comparative Study of Box-Behnken, Central Composite, and Doehlert Matrix for Multivariate Optimization of Pb (II) Adsorption onto Robinia Tree Leaves. *Journal of Chemometrics*. 27(1–2): 12–20. <https://doi.org/10.1002/cem.2487>.
- [20] Berkani, M., Y. Kadmi, M. K. Bouchare, M. Bouhelassa, and A. Bouzaza. 2020. Combination of a Box-Behnken Design Technique with Response Surface Methodology for Optimization of the Photocatalytic Mineralization of C.I. Basic Red 46 Dye from Aqueous Solution. *Arabian Journal of Chemistry*. 13(11): 8338–8346. <https://doi.org/10.1016/j.arabjc.2020.05.013>.
- [21] Homkhiew, C., W. Boonchouytan, W. Cheewawuttipong, L. Buppapo, P. Auttagomsakun, and T. Ratanawilai. 2018. Effects of Extruding Factors on Mechanical and Physical Properties of Polypropylene/Rubberwood Flour Composites. *Engineering and Applied Science Research*. 45(2): 120–126.
- [22] Homkhiew, C., W. Boonchouytan, W. Cheewawuttipong, N. Hoysakul, W. Kaewkong, and T. Ratanawilai. 2020. Measurement in Some Properties of Non-Toxic Particleboard to Optimize the Formulation for Food Containers. *Measurement*. 156: 107617. <https://doi.org/10.1016/j.measurement.2020.107617>.
- [23] Alaba, E. S., R. A. Kazeem, A. S. Adebayo, M. O. Petinrin, O. M. Ikumapayi, T. C. Jen, and E. T. Akinlabi. 2023. Evaluation of Palm Kernel Oil as Cutting Lubricant in Turning AISI 1039 Steel Using Taguchi-Grey Relational Analysis Optimization Technique. *Advances in Industrial and Manufacturing Engineering*. 6: 100115. <https://doi.org/10.1016/j.aime.2023.100115>.
- [24] Homkhiew, C., T. Ratanawilai, and W. Thongruang. 2015. Minimizing the Creep of Recycled Polypropylene/Rubberwood Flour Composites with Mixture

- Design Experiments. *Journal of Composite Materials*. 49(1): 17–26. <https://doi.org/10.1177/0021998313514257>.
- [25] Tan, Y., X. Yu, X. Wang, Q. Lv, and M. Shi. 2022. Interaction Analysis and Multi-Response Optimization of Transformer Winding Design Parameters. *International Communications in Heat and Mass Transfer*. 137: 106233. <https://doi.org/10.1016/j.icheatmasstransfer.2022.106233>.
- [26] Petdee, T., T. Naemsai, C. Homkhiew, and E. Pianhanuruk. 2023. Multiple Response Optimization of Wood Sawdust/Natural Rubber Foam Composites for Stair Tread Covers. *Industrial Crops and Products*. 204: 117312. <https://doi.org/10.1016/j.indcrop.2023.117312>.
- [27] Srivabut, C., S. Rawangwong, S. Hiziroglu, and C. Homkhiew. 2024. Multi-Objective Optimization of Turning Process Parameters and Wood Sawdust Contents Using Response Surface Methodology for the Minimized Surface Roughness of Recycled Plastic/Wood Sawdust Composites. *Composites Part C: Open Access*. 14: 100477. <https://doi.org/10.1016/j.jcomc.2024.100477>.
- [28] Myers, R. H., D. C. Montgomery, and C. M. Anderson-Cook. 2009. *Response Surface Methodology: Process and Product Optimization Using Designed Experiments*. 3rd ed. New York: John Wiley & Sons.
- [29] Koli, Y., N. Yuvaraj, S. Aravindan, and Vipin. 2021. Multi-Response Mathematical Model for Optimization of Process Parameters in CMT Welding of Dissimilar Thickness AA6061-T6 and AA6082-T6 Alloys Using RSM-GRA Coupled with PCA. *Advances in Industrial and Manufacturing Engineering*. 2: 100050. <https://doi.org/10.1016/j.aime.2021.100050>.
- [30] Montgomery, D. C. 2019. *Design and Analysis of Experiments*. 10th ed. New York: John Wiley & Sons.
- [31] Kumar, S., R. Singh, and N. S. Maurya. 2023. Modelling of Corrosion Rate in the Drinking Water Distribution Network Using Design Expert 13 Software. *Environmental Science and Pollution Research*. 30: 45428–45444. <https://doi.org/10.1007/s11356-023-25465-z>.
- [32] Homkhiew, C., W. Boonchouytan, S. Rawangwong, and T. Ratanawilai. 2017. Optimal Manufacturing Parameters of Rubberwood Flour/High Density Polyethylene Composites Using Box-Behnken Design. *The Journal of King Mongkut's University of Technology North Bangkok*. 27(2): 315–328.
- [33] Nonaka, S., K. Umemura, and S. Kawai. 2013. Characterization of Bagasse Binderless Particleboard Manufactured in High-Temperature Range. *Journal of Wood Science*. 59: 50–56. <https://doi.org/10.1007/s10086-012-1302-6>.
- [34] Gopalakannan, S., and T. Senthilvelan. 2013. Application of Response Surface Method on Machining of Al-SiC Nano-Composites. *Measurement*. 46(8): 2705–2715. <https://doi.org/10.1016/j.measurement.2013.04.036>.
- [35] Yaghoobi, H., and A. Fereidoon. 2018. Modeling and Optimization of Tensile Strength and Modulus of Polypropylene/Kenaf Fiber Biocomposites Using Box-Behnken Response Surface Method. *Polymer Composites*. 39(S1): E463–E479. <https://doi.org/10.1002/pc.24596>.